Doubly differential cross sections of secondary electrons ejected from gases by electron impact: 50–400 eV on N_2

T. W. Shyn
Space Physics Research Laboratory, University of Michigan, Ann Arbor, Michigan 48109
(Received 15 December 1982)

Doubly differential cross sections of secondary electrons ejected from N_2 by electron impact have been measured by a crossed-beam method. The incident energies used were 50, 70, 100, 200, and 400 eV. The energy and angular range of secondary electrons measured were from 1.0 eV to one-half of the difference between the incident energy and ionization potential and 12° to 156°, respectively. The present results have been compared with two previous measurements and considerable discrepancies were found.

I. INTRODUCTION

Total ionization cross sections of N_2 by electron impact have been measured by Tate and Smith,[1] Rapp and Englander-Golden,[2] and Schram *et al.*[3] The doubly differential cross sections (DDCS) of secondary electrons from N_2 have been measured by Opal *et al.*[4] and DuBois and Rudd.[5] The energy and angular range of secondary electrons in the measurements of Opal *et al.* were from 4 eV to one-half the incident energy and from 30° to 150°, respectively. The range of incident energy used was from 50 to 2000 eV. DuBois and Rudd had an energy range of secondary electrons from 4 eV to the difference between the incident energy and ionization potential, and an angular range of 10°–150°. The incident energies used were 100, 250, and 500 eV. Neither measurements covered the low-energy range of the secondary electrons below 4 eV from where a large fraction (as much as 50%) of the ionization cross section comes, and they do not agree with each other in the shape of the DDCS's of the secondary electrons as well as the magnitude of the differential cross section and the total ionization cross sections. Both measurements mentioned above include dissociative ionizations (N^+) in addition to the direct-ionization cross sections ($N_2{}^+$, $N_2{}^{2+}$, etc.). Crowe and McConkey[6] have measured the dissociative and single ionization cross sections of N_2 separately by electron impact. The incident energies used were from 50 to 300 eV.

This paper presents results of experiments in which the DDCS's of secondary electrons ejected from N_2 have been measured by electron impact utilizing a cross-beam method. The energy and angular range of secondary electrons measured were from 1.0 eV to one-half of the difference between incident energy and ionization potential and from 12° to 156°, respectively. The incident energies used were from 50 to 400 eV.

II. APPARATUS AND PROCEDURE

The apparatus used for the present measurements is the same as that used previously for the measurements of secondary electrons ejected from He,[7] CO_2,[8] and H_2.[9] A detailed description of the apparatus can be found elsewhere.[7,10] Briefly, the apparatus consists of three subsystems: a rotatable electron-beam monochromator, a neutral beam collimated by a fused capillary array, and an electron detector fixed on the vacuum chamber wall. The rotatable electron beam of a certain energy in a horizontal plane intersects with the vertically collimated neutral beam at 90° in the interaction region. The ejected electrons from the neutral beam are detected by an electron channeltron multiplier after energy analysis by 127° electrostatic energy analyzer. When the neutral beam of N_2 was on the background, pressure rose to 2×10^{-5} Torr and the density of the beam in the interaction region was estimated to be three times larger than the background density.

The stray magnetic fields in the plane of the measurements have been reduced to less than 10 mG in all directions by three orthogonal Helmholtz coils. The absolute energy scale was calibrated frequently to within 0.05 eV with the use of the He resonance at 19.3 eV.

The procedure used to measure the DDCS is as follows: the collimated neutral beam of N_2 is turned on and the signal count is integrated for 10 sec for each angle from 12° to 156° in 12° increments for selected incident and secondary energy. The measurements are repeated with the gas beam off to ob-

TABLE I. DDCS ($d^2\sigma/d\Omega\, dE$) of secondary electrons ejected from N_2 by 50-eV electron impact (in units of 10^{-19} $cm^2/sr\,eV$). (The numbers in parentheses represent extrapolated data points.)

E_s (eV) \ θ°	12	24	36	48	60	72	84	96	108	120	132	144	156	168	$\Delta\sigma/\Delta E$ (10^{-18} cm^2/eV)
1.0	62.8	18.8	8.31	8.12	7.91	11.3	11.7	13.8	16.2	17.3	16.2	14.0	12.9	(11.5)	17.5
2.0	41.3	19.0	11.3	11.2	10.7	13.7	13.5	14.3	14.7	15.0	14.3	13.4	12.5	(11.6)	17.8
3.0	33.9	19.0	13.9	14.1	11.0	12.4	12.0	11.9	12.4	13.1	13.8	13.3	12.8	(12.5)	16.8
4.0	31.0	16.6	14.3	10.4	10.6	11.2	10.9	10.8	11.2	12.0	12.9	13.5	13.2	(13.5)	15.8
5.0	28.4	15.2	13.4	13.6	10.6	10.8	10.3	10.2	10.8	11.3	12.5	13.2	13.7	(14.6)	15.2
6.0	19.1	13.7	11.9	13.0	10.1	10.2	9.96	9.84	10.1	11.0	12.2	13.1	13.7	(14.3)	14.3
8.0	17.0	14.1	11.8	11.6	9.50	9.23	8.28	8.26	8.67	9.24	10.3	11.6	13.1	(14.6)	12.8
10.0	18.7	14.1	11.7	10.5	8.82	8.14	7.51	7.31	7.53	8.18	9.34	10.7	12.0	(13.3)	11.7
12.0	18.9	16.1	12.9	11.1	9.13	7.66	6.72	6.60	7.14	7.86	9.11	10.5	12.1	(13.6)	11.7
15.0	20.7	17.0	11.9	9.42	7.57	5.93	5.44	5.35	5.77	6.74	7.81	9.11	10.5	(11.9)	10.1
17.2	21.8	15.8	10.7	8.22	6.39	5.08	4.55	4.50	4.96	5.79	6.87	7.95	9.24	(11.5)	9.0

TABLE II. DDCS ($d^2\sigma/d\Omega\, dE$) of secondary electrons ejected from N_2 by 70-eV electron impact (in units of 10^{-19} $cm^2/sr\,eV$). (The numbers in parentheses represent extrapolated data points.)

E_s (eV) \ θ°	12	24	36	48	60	72	84	96	108	120	132	144	156	168	$\Delta\sigma/\Delta E$ (10^{-18} cm^2/eV)
1.0	39.5	25.4	18.9	13.2	11.3	12.3	17.9	22.6	22.6	27.3	29.1	22.6	21.6	(18.9)	21.8
2.0	26.9	19.2	18.1	17.2	14.0	17.2	17.8	17.8	19.6	19.2	19.6	20.0	20.0	(19.9)	20.5
3.0	26.6	17.1	19.3	16.8	13.4	13.7	14.3	14.0	15.0	15.3	16.2	16.5	18.3	(19.8)	18.4
4.0	22.6	15.5	16.7	16.4	13.6	14.0	13.7	12.9	14.3	15.0	15.5	17.1	18.7	(20.0)	17.5
5.0	18.0	13.9	12.9	13.4	11.8	12.2	12.6	11.8	12.3	13.2	13.5	14.3	16.8	(19.3)	15.4
6.0	18.9	13.3	13.6	14.6	11.6	12.3	11.7	11.1	11.5	11.8	13.0	14.0	15.3	(16.5)	15.0
8.0	15.8	13.3	13.7	11.4	9.00	9.50	8.88	8.46	8.88	9.30	9.99	11.5	13.0	(14.4)	12.8
10.0	18.6	16.1	13.3	12.2	11.2	9.71	8.05	7.77	8.05	8.46	9.71	11.2	12.3	(13.3)	12.2
12.0	19.7	14.6	13.6	12.8	10.4	8.33	6.80	6.52	6.80	7.49	8.60	10.1	11.4	(12.8)	11.3
15.0	14.9	12.2	10.7	8.74	7.08	5.82	4.72	4.44	4.72	5.27	6.24	7.22	8.05	(8.74)	8.00
20.0	13.0	10.3	7.40	6.11	4.58	4.02	3.33	3.05	3.19	3.61	4.44	4.85	5.82	(6.80)	5.64
27.2	14.6	10.1	6.38	4.58	3.33	2.64	2.22	1.94	1.94	2.36	2.91	3.61	4.44	(5.13)	4.38

tain the background counts. The difference between the two signals DDCS of secondary electrons ejected from the N_2 beam.

The correction of the final data for the path-length effect due to the background density has been made. The contribution of the background density to total signal has been measured at 90° to be $(34\pm2)\%$.

III. EXPERIMENTAL RESULTS

The DDCS of secondary electrons have been measured at the incident energies of 50, 70, 100, 200, and 400 eV. The results have been calibrated among themselves by normalizing the scattered signal against the incident electron current and target density for each incident and secondary electron energy. The normalized results have been placed on an absolute scale using the elastic cross sections of N_2 at 50 eV measured by Shyn and Carignan.[11]

The statistical uncertainty of data points is less than 4% except for the secondary energies less than 3 eV at small angles ($<24°$). The upper limit of the uncertainty at 12° was estimated to be 15%. There is 7% uncertainty in intersecondary electron energy calibration and 6% in interincident energy calibration. The normalization process of the present result to the elastic cross sections of N_2 at 50 eV including the uncertainty in N_2 elastic cross sections ($\pm14\%$) contains $\pm15\%$ uncertainty. The path-length correction has 2% uncertainty except at 12°. Thus the resultant uncertainty of the present result is $\pm18\%$.

Absolute cross sections of DDCS for five incident energies measured are shown in Tables I–V. The present results contain the contributions from dissociative ionization, single ionization, and multiple ionizations.

Figure 1 shows a three-dimensional perspective diagram of secondary electrons ejected from N_2 by 200-eV electron impact. Below 20 eV of secondary energies, angular distributions are nearly isotropic except for very low energies (<5 eV) where there is a strong forward scattering. It is noted, however, that the backward scattering stays nearly constant from 1 to 12 eV of secondary electron energy and decreases gradually as the second energy increases. There is an increase in the scattering signal near 60° above 40 eV and this is due to the momentum and energy conservation of the colliding system.

Figure 2 shows the DDCS of 4.0 eV secondary electron at 50-eV electron impact along with the result of Opal *et al.* Agreement between the present result and that of Opal *et al.* is relatively good near 90° and very poor at extreme angles. This may be

TABLE III. DDCS ($d^2\sigma/d\Omega\,dE$) of secondary electrons ejected from N_2 by 100-eV electron impact (in units of 10^{-20} cm^2/sr eV). (The numbers in parentheses represent extrapolated data points.)

E_s (eV) \ $\theta°$	12	24	36	48	60	72	84	96	108	120	132	144	156	168	$\Delta\sigma/\Delta E$ (10^{-18} cm^2/eV)
1.0	592.7	205.3	102.7	95.8	99.2	112.9	119.8	126.6	171.1	205.3	198.5	171.1	136.9	(112.9)	20.44
2.0	483.9	207.5	135.9	127.4	129.9	133.5	129.3	145.0	149.8	140.0	135.0	133.1	125.0	(120.0)	18.29
3.0	365.8	231.8	162.4	156.4	126.1	134.0	130.4	129.2	128.6	136.4	145.5	138.8	129.8	(123.7)	18.03
4.0	330.6	193.9	156.9	158.8	123.2	130.4	125.1	120.3	122.2	130.4	137.6	134.8	133.8	(129.9)	17.11
5.0	266.7	202.7	159.5	148.1	118.6	119.8	113.9	110.4	112.0	116.3	123.0	127.3	133.2	(137.5)	16.08
6.0	199.0	153.8	144.6	135.2	105.1	106.4	102.5	99.4	101.6	104.8	112.7	119.7	127.7	(133.7)	14.51
8.0	174.4	138.1	126.1	126.3	105.7	98.7	91.2	86.0	83.0	87.0	93.4	102.7	111.1	(119.4)	12.84
10.0	148.4	123.1	109.6	98.3	83.9	74.2	70.2	69.8	69.1	73.2	77.8	86.9	96.4	(105.7)	10.50
12.0	117.1	115.6	102.6	96.6	81.9	74.3	64.8	59.8	59.1	62.9	69.4	77.6	86.7	(95.8)	9.55
15.0	100.0	98.0	89.0	72.6	62.4	50.3	42.9	38.7	40.2	45.3	51.2	57.5	64.9	(72.6)	7.12
20.0	94.5	78.2	59.9	49.5	41.5	35.1	29.1	26.7	27.1	30.9	34.0	39.5	45.6	(51.7)	4.98
25.0	67.1	56.3	40.6	33.9	27.4	21.8	18.2	16.5	16.5	17.2	21.1	25.6	29.8	(33.9)	3.22
30.0	59.6	41.6	32.1	25.5	18.6	15.3	12.9	11.7	11.6	13.2	15.4	19.1	23.5	(28.0)	2.40
35.0	69.5	44.9	30.7	22.9	15.9	12.6	10.4	9.44	9.52	11.1	13.7	17.7	21.4	(25.1)	2.20
40.0	84.0	52.1	32.1	23.0	16.3	11.3	9.00	8.21	8.54	10.0	12.7	16.1	20.6	(25.2)	2.18
42.2	94.7	55.5	33.3	22.4	15.2	10.7	8.34	7.63	8.03	9.83	12.4	16.0	20.3	(24.6)	2.18

TABLE IV. DDCS ($d^2\sigma/d\Omega\, dE$) of secondary electrons ejected from N_2 by 200-eV electron impact (in units of 10^{-20} $cm^2/sr\, eV$). (The numbers in parentheses represent extrapolated data points.)

E_s (eV) \ $\theta°$	12	24	36	48	60	72	84	96	108	120	132	144	156	168	$\Delta\sigma/\Delta E$ (10^{-18} cm^2/eV)
1.0	930.0	305.8	211.1	113.8	80.3	82.0	85.4	73.7	75.4	83.7	83.7	70.3	(64.0)	(58.0)	14.5
2.0	580.0	221.9	108.7	86.9	87.1	91.2	81.2	89.5	96.4	96.4	92.9	88.6	(74.0)	(67.0)	13.0
3.0	442.2	197.8	113.1	109.4	97.3	98.0	89.0	92.0	92.0	93.2	88.5	79.5	74.0	(66.0)	12.6
4.0	355.0	178.9	126.2	113.8	94.1	99.2	94.1	91.4	91.9	94.7	87.0	80.0	71.0	(62.0)	12.0
5.0	300.2	143.7	121.4	103.7	86.1	88.1	82.5	79.8	79.0	79.8	79.0	73.4	67.1	(63.8)	11.2
6.0	226.7	117.2	100.6	100.1	80.6	78.5	76.2	71.8	70.6	71.3	71.5	68.3	68.4	(68.4)	10.3
8.0	175.7	103.6	89.0	86.6	74.2	73.2	67.6	63.3	58.8	60.4	61.0	62.8	63.0	(63.2)	9.09
10.0	106.5	85.9	81.8	77.4	71.5	66.2	60.1	55.9	53.2	55.9	54.5	56.5	60.4	(64.5)	7.95
12.0	97.8	82.2	71.8	73.4	63.5	58.8	53.1	48.6	45.0	45.7	46.4	48.7	50.8	(52.6)	6.98
15.0	66.9	59.1	55.4	53.5	48.6	45.0	40.9	36.8	34.3	34.3	35.1	37.2	39.4	(41.6)	5.36
20.0	56.4	45.2	38.4	34.5	31.2	27.5	24.3	21.2	19.9	19.5	20.9	23.1	25.5	(27.8)	3.40
25.0	54.5	42.1	36.8	28.2	23.8	19.4	16.1	14.3	12.9	12.9	13.9	16.3	18.7	(21.1)	2.60
30.0	38.5	30.6	24.1	19.9	17.7	14.6	11.9	9.84	8.83	8.66	9.51	10.9	12.6	(14.4)	1.81
35.0	26.2	21.6	16.3	14.8	13.1	11.0	8.49	6.96	6.45	6.28	6.62	7.64	9.17	(10.7)	1.31
40.0	19.2	13.6	11.5	11.2	10.2	8.32	6.45	5.43	4.75	4.75	5.26	5.77	6.62	(7.47)	0.97
50.0	14.3	9.34	7.98	8.15	7.13	5.26	3.91	3.23	2.92	3.02	3.36	3.91	4.41	(5.09)	0.64
65.0	12.7	8.66	6.79	6.28	4.92	3.06	2.21	1.87	1.70	1.80	2.07	2.38	2.80	(3.23)	0.45
80.0	15.5	9.34	6.96	5.60	3.57	2.29	1.56	1.34	1.19	1.34	1.60	1.95	2.31	(2.66)	0.39
92.2	19.0	11.5	7.64	5.09	2.97	1.85	1.29	1.14	1.10	1.17	1.39	1.70	2.00	(2.33)	0.38

TABLE V. DDCS ($d^2\sigma/d\Omega\, dE$) of secondary electrons ejected from N_2 by 400-eV electron impact (in units of 10^{-20} $cm^2/sr\,eV$). (The numbers in parentheses represent extrapolated data points.)

E_s (eV) \ $\theta°$	12	24	36	48	60	72	84	96	108	120	132	144	156	168	$\Delta\sigma/\Delta E$ (10^{-18} cm^2/eV)
1.0	701.1	287.2	205.8	71.0	48.0	38.2	34.3	28.4	29.6	38.0	40.3	30.8	24.8	(19.0)	9.09
2.0	502.2	113.0	89.0	69.0	53.5	50.6	42.0	48.5	51.3	59.6	52.1	32.2	24.5	(17.6)	8.63
3.0	366.0	125.1	75.6	74.0	59.9	60.3	53.2	56.9	58.0	52.8	46.4	33.3	22.5	(16.9)	8.06
4.0	284.7	122.6	80.2	77.0	55.0	55.0	51.4	51.1	49.2	49.4	43.8	32.1	21.2	(15.6)	7.44
5.0	221.4	91.6	72.7	70.3	52.9	54.1	52.9	51.2	51.4	48.4	43.7	35.4	26.0	(19.4)	7.06
6.0	187.3	88.3	71.9	67.5	55.5	51.8	50.1	46.2	46.2	44.9	38.0	30.7	21.5	(16.4)	6.51
8.0	123.3	69.6	58.7	57.9	47.8	46.3	44.7	42.6	39.5	36.7	34.4	28.6	23.5	(20.1)	5.64
10.0	96.8	55.9	46.0	47.4	47.3	45.2	40.6	37.7	34.5	32.3	30.0	27.1	26.6	(26.0)	5.03
12.0	72.6	52.4	45.8	46.3	43.3	43.4	37.2	32.9	30.2	28.8	27.9	27.6	27.2	(26.7)	4.61
15.0	47.1	35.7	34.8	35.7	31.9	30.3	27.6	25.0	22.9	21.6	20.7	21.0	21.4	(22.0)	3.44
20.0	27.8	21.0	20.8	21.0	19.5	18.3	16.9	15.0	14.2	12.2	12.0	12.6	13.0	(13.3)	2.06
25.0	21.4	16.3	15.0	15.1	14.1	13.2	11.8	10.1	9.3	7.9	7.6	8.1	8.8	(9.5)	1.43
30.0	13.9	11.6	10.8	11.0	11.0	10.3	8.9	7.3	6.1	5.4	5.4	5.5	6.1	(6.8)	1.04
35.0	12.9	10.2	8.7	8.8	8.6	7.9	6.8	5.5	4.6	4.2	4.0	4.4	4.8	(5.2)	0.82
40.0	11.3	8.8	7.1	7.2	7.2	6.4	5.3	4.2	3.5	3.1	3.1	3.5	3.7	(4.3)	0.66
50.0	6.7	4.9	4.3	4.6	4.8	4.2	3.1	2.5	1.9	1.8	1.7	2.1	2.3	(2.5)	0.40
65.0	4.4	2.8	2.5	3.0	3.0	2.5	1.7	1.2	0.99	0.94	1.0	1.1	1.3	(1.4)	0.23
80.0	3.6	2.2	1.8	2.2	2.2	1.7	1.1	0.74	0.62	0.56	0.61	0.72	0.83	(0.96)	0.16
100.0	3.2	1.8	1.2	1.8	1.5	1.1	0.65	0.47	0.37	0.33	0.37	0.45	0.47	(0.50)	0.11
120.0	2.8	1.4	1.2	1.4	1.3	0.75	0.42	0.28	0.28	0.27	0.29	0.33	0.36	(0.39)	0.086
140.0	2.9	1.5	1.2	1.3	0.92	0.55	0.36	0.29	0.26	0.26	0.22	0.28	0.32	(0.34)	0.077
160.0	2.69	1.39	1.22	1.14	0.80	0.50	0.34	0.26	0.23	0.23	0.22	0.24	0.26	(0.29)	0.070
180.0	2.45	1.56	1.19	0.96	0.66	0.54	0.33	0.26	0.22	0.21	0.21	0.24	0.23	(0.22)	0.065
192.2	2.84	1.43	1.14	0.88	0.60	0.41	0.29	0.25	0.23	0.21	0.24	0.22	0.26	(0.28)	0.063

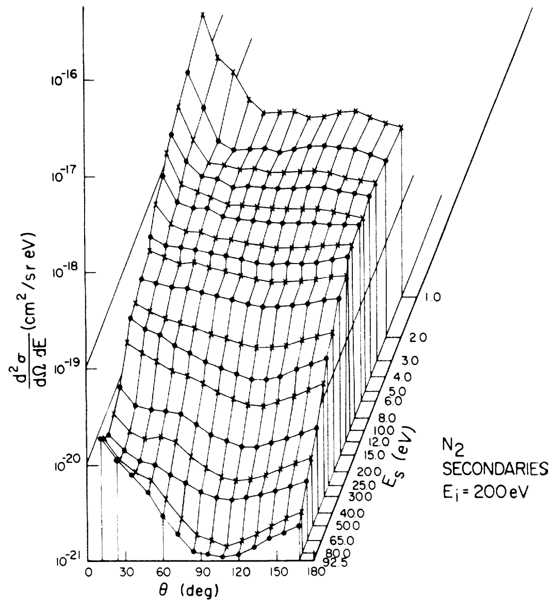

FIG. 1. Three-dimensional perspective diagram of secondary electrons ejected from N_2 at 200-eV incident energy.

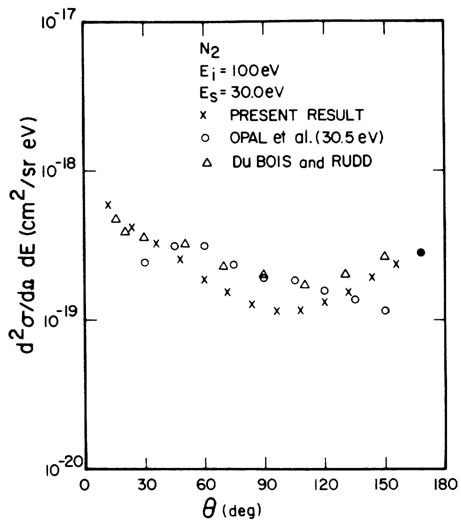

FIG. 3. DDCS of 30-eV secondary electrons ejected from N_2 at 100-eV incident energy along with those of Opal *et al.* and DuBois and Rudd.

due to the overcorrection of path-length effect on the results of Opal *et al.*

Figure 3 shows the DDCS of 30 eV of secondary electrons ejected from N_2 at 100-eV electron impact along with the results of Opal *et al.* and DuBois and Rudd. The results of Opal *et al.* have the same trend described in Fig. 2 except for the larger DDCS than the present results. The result of DuBois and Rudd agrees with the present results at extreme angles, however, their results are larger near 90° than the present results.

Singly differential cross sections (SDCS) at 50-eV electron impact along with the results of Opal *et al.* are shown in Fig. 4. The general shape of the results of Opal *et al.* agrees with those of the present results, but the absolute magnitude is smaller than the present results by 50%, approximately. Figure 5 shows SDCS at 100-eV electron impact along with the results of Opal *et al.* and that of DuBois and

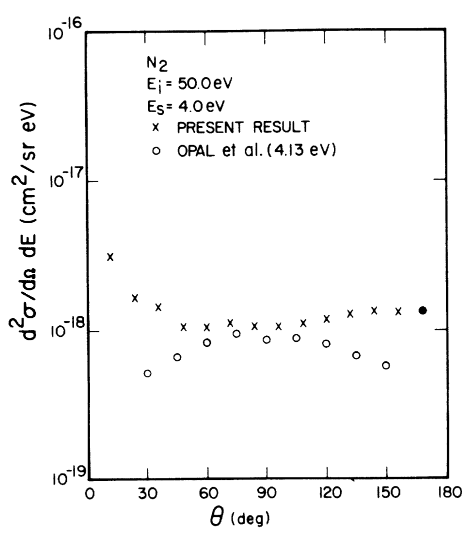

FIG. 2. DDCS of 4.0-eV secondary electrons ejected from N_2 at 50-eV incident energy (dot is an extrapolated data point) along with those of Opal *et al.*

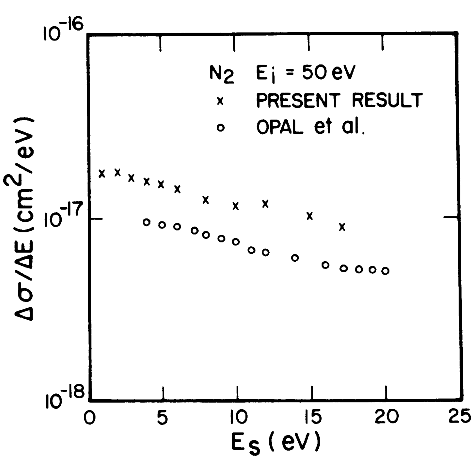

FIG. 4. Singly differential cross section of secondary electrons ejected from N_2 at 50-eV incident energy along with those of Opal *et al.*

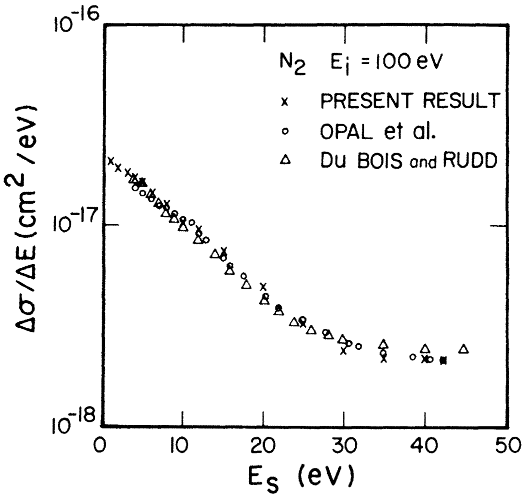

FIG. 5. Singly differential cross section of secondary electrons ejected from N_2 at 100-eV electron impact along with those of Opal *et al.* and DuBois and Rudd.

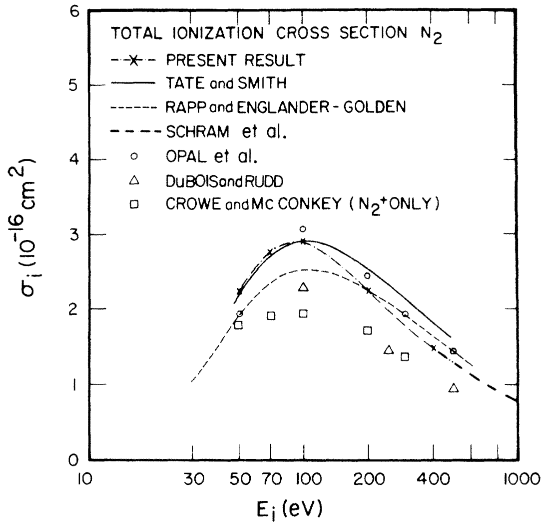

FIG. 6. Total ionization cross section of N_2 along with the previous measurements.

Rudd. The agreement among the three measurements is generally good in shape and magnitude.

Figure 6 shows the total ionization cross sections of the present experiment along with other measurements. The results of Tate and Smith agree with the present results very well below 100 eV and, however, above 100 eV their results are larger than the present results by 10%, approximately. The results of Schram *et al.* are in a right trend in shape and magnitude with the present results above 400 eV. The results of Opal *et al.* agree well with the present results except a low-energy impact (50 eV). The value at the low energy incident is smaller than the present result by 10% approximately. The results of Rapp and Englander-Golden show smaller values below 200 eV and larger values above 200 eV than the present results. The results of DuBois and Rudd are substantially smaller than the present results (more than 25%). Crowe and McConkey have measured only N_2^+ cross sections, and the difference between their results and the present measurement is about 30% at 100-eV incident energy and smaller at other incident energies. This may imply that this 30% is the sum of a multiple ionization cross section and dissociative ionization cross section at 100-eV incident energy.

Finally, Fig. 7 shows the Platzman plot of the present results along with semitheoretical results analyzed by Kim.[12] The detailed explanation and advantage of the Platzman plot can be found elsewhere.[12,13] Briefly, the ordinate of the plot is the ratio of the singly differential cross section to the Rutherford cross section $Y(E)$, and the abscissa is the ratio of R, the Rydberg constant, to E, the energy transfer. In this plot, $Y(E)$ approaches the effective number of electrons participating in the ionization process for large transferred energy and $Y(E)$ also resembles $E(df/dE)$ in shape for small E, where (df/dE) is the density of the dipole oscillator strength for ionization. The Platzman plot is very effective in checking the consistency for experimental data on secondary electrons.

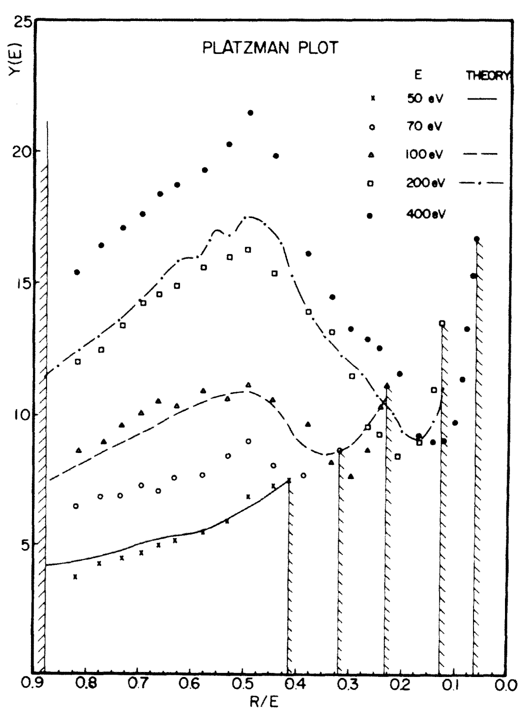

FIG. 7. Platzman plot.

Agreement between the present result and Kim's analysis which is based on the Born approximation is generally good except near the middle of the energy region. This may be due in part to inadequacy of the Born approximation in the low-energy region.

ACKNOWLEDGMENT

This work was supported by the National Science Foundation, Atmospheric Research Section, Grant No. ATM-81-05022.

[1]J. T. Tate and P. T. Smith, Phys. Rev. 39, 270 (1932).
[2]D. Rapp and P. Englander-Golden, J. Chem. Phys. 43, 1464 (1965).
[3]B. L. Schram, F. J. de Hoer, M. J. Van der Wiel, and J. Kistemaker, Physica (Utrecht) 31, 94 (1964).
[4]C. B. Opal, E. C. Beaty, and W. K. Peterson, At. Data 4, 209 (1972).
[5]R. D. DuBois and M. E. Rudd, Phys. Rev. A 17, 843 (1978).
[6]A. Crowe and J. W. McConkey, J. Phys. B 6, 2108 (1973).
[7]T. W. Shyn and W. E. Sharp, Phys. Rev. A 19, 557 (1979).
[8]T. W. Shyn and W. E. Sharp, Phys. Rev. A 20, 2322 (1979).
[9]T. W. Shyn, W. E. Sharp, and Y. K. Kim, Phys. Rev. A 24, 79 (1981).
[10]T. W. Shyn, R. S. Stolanski, and G. R. Carignan, Phys. Rev. A 6, 1002 (1972).
[11]T. W. Shyn and G. R. Carignan, Phys. Rev. A 22, 923 (1980).
[12]Y. K. Kim, Radiat. Res. 64, 96 (1975).
[13]Y. K. Kim, Radiat. Res. 61, 21 (1975).